Article

Development of Adjustable High-Voltage Power Supply for Air Kerma Meter

Jinxing Cheng[1*], Qiu Huang[2], Qingbo Wang[1], Ai Yu[1], Weiwei Wen[1], Youpeng Wu[1], Jian Yang[2], Xinyu Li[3],Fang Liu[4], Yue Zhang[1], Zeqian Wu[5] and Changwei Zhao[6]

[1] Beijing New-High Technology Academy, Beijing, 100094,China; chengjx@tsinghua.org.cn; wqb08@tsinghua.org.cn; yuai@novelmedical.cn; wenweiwei@novelmedical.cn; wuyoupeng@novelmedical.cn; zhangyue@novelmedical.cn
[2] Radiation Research Institute of National Institute of Measurement and Testing Technology, Chengdu, Sichuan 610021,China; huangqiu@nimtt.com; yangjian@nimtt.com
[3] Chengdu University of Technology, Chengdu, Sichuan 610059,China;937121251@nimtt.com
[4] North China Electric Power University, Beijing 102206,China; liuf@ncepu.edu.cn
[5] Institute of NBC defence, Beijing 102205, China; wuzeqian@novelmedical.cn
[6] College of Resources and Environmental Sciences, China Agricultural University, Beijing 100193, China; 1804762788@qq.com
* Correspondence: chengjx@tsinghua.org.cn

Abstract: The general circuit topology and principles of low-noise high-voltage power supply are investigated to meet the requirements of the high-voltage bias application in air kerma meters. Two topologies, flyback converter and Royer converter are simulated using SPICE simulation program. The simulation results indicate that the circuit structure of the Royer converter is more complex, but it obtains lower output high voltage noise. While we develop an adjustable high-voltage power supply according to the circuit structure of the Royer converter, and tested it to ensure the design requirements for continuously adjustable output high-voltage linearity. The test results show that the linear adjustment rate is not more than ±0.0025%, the load regulation rate is less than ±0.1%, and the output ripple noise voltage percentage is less than 0.01%. These tested performance make it more suitable for accurate nuclear measurements.

Keywords: air kerma meter; flyback converter; high-voltage power supply; Royer converter

1. Introduction

The air kerma meter is a radiation meter used to measure the air kerma produced by an external radiation source [1]-[4]. It is usually composed of several major parts for detection, signal processing, analysis, display, output, etc., of which the most important part that determines the basic performance of the meter is the detector. The frequently-used nuclear radiation detectors such as gas detectors, scintillation detectors, semiconductor detectors, solid-state trace detectors, etc., require using a high-voltage power supply as the detection bias voltage [5][6]. Therefore, the accuracy of nuclear radiation detectors that require high-voltage bias depends on the performance of the high-voltage power supply. The main indicators of interest for the high-voltage power supply of air kerma meters include output voltage linearity, linearity regulation, load regulation, output ripple and noise, etc.

The high-voltage power supply module commonly used in radiation monitoring instruments shall not exceed 10 W at most, which belongs to micro power supply. Push pull converter and flyback converter are usually selected to achieve high-voltage output. In the research on high voltage of nuclear instruments, Masatosi Imori et al. designed a high voltage source with 1500V to 2000V output using driver circuits, transformers and Cockcroft-Walton circuits for the high voltage of photomultiplier tubes[7]. It has a load resistance of more than 10 MΩ and a conversion efficiency of more than 50%. Zeng Guoqiang and others designed a DC high-voltage power supply for the ionization chamber

Preprints (www.preprints.org) | NOT PEER-REVIEWED | Posted: 29 December 2022 doi:10.20944/preprints202212.0553.v1

according to the Royer principle [8]. In this method, two triodes are used to generate self-excited oscillation, then high-voltage output is obtained through transformer, and finally DC high-voltage output is obtained through rectification. Its output voltage can reach 3kV, and the feedback part adopts switching regulator TL1534. This method has low noise and high conversion efficiency. Qiang Guo et al. designed a programmable high-voltage power supply module for nuclear instruments based on the flyback converter principle [9]. Flyback converter is a kind of switching power supply, the switching signal is controlled by PWM. Its output voltage is 0 to 600V, and the power supply noise does not exceed 600mV. Yu Qianqian and Qiao Minjuan et al. also designed DC high-voltage power supply in the context of nuclear instrument application [10], [11]. Both of them are low noise and low power.

In order to improve the performance of nuclear radiation detectors and ensure their compliance with higher requirements for air kerma measurement, an adjustable high-voltage power supply for air kerma meter is developed and proposed in this paper. The test results for the developed adjustable high-voltage power supply show that the key parameters including linear adjustment rate, the load regulation rate and the output ripple noise voltage percentage can meet well with the accurate nuclear measurements for air kerma meter.

2. Basic Circuit Principle

The indicators of high-voltage power supply are closely related to circuit topology and design, and the ripple and noise are of particular importance as they restrain the limits of detector measurement, and the power supply topology largely determines the size of the ripple and noise [12]. The output current of the high-voltage power supply for air kerma meters is generally less than 10 mA, and its applicable topological structures are the flyback converters and the Royer converter.

2.1. Circuit Principle of Flyback Converter

The basic circuit of a flyback converter shown in Fig. 1 operates as follows: when Q1 is conducting, rectifier diode D1 is subject to reverse cut-off, and output capacitor C1 supplies power to load R1. Transformer T1 is equivalent to a pure inductor, Vin is added to both ends, and the current flowing through transformer primary winding Np rises linearly to a peak of I max. When Q1 is turned off, the voltage of transformer secondary winding Ns is reversed, and the reverse voltage causes the rectifier diode to enter the conducting state, while all or part of the energy stored in the primary winding $\frac{1}{2}L_pI_{max}{}^2$ is transferred to the secondary winding to provide load current and charge output capacitor C1[13],[14].

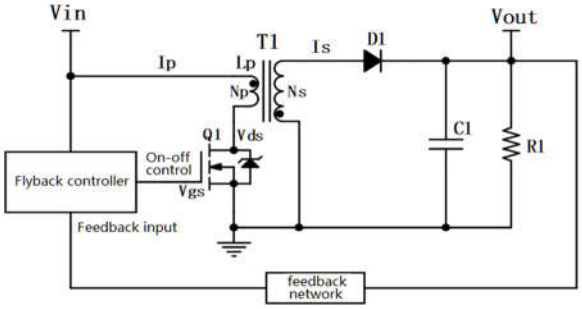

Figure 1. Basic circuit block diagram of flyback converter.

The flyback converter output is not connected to a filter inductor and does not require a high-voltage freewheel diode, giving this topology great advantages in high-voltage output. However, the large secondary peak current at the instant that the switch tube is turned off can cause serious RFI problems and high output noise[15]-[17].

Preprints (www.preprints.org) | NOT PEER-REVIEWED | Posted: 29 December 2022 doi:10.20944/preprints202212.0553.v1

2.2. Circuit Principle of Royer Converter

The basic circuit of a Royer converter, as shown in Fig. 2, is mainly composed of a pair of push-pull Negative-Positive-Negative (NPN) triodes, multi-winding transformer, rectifier diode, filter capacitor, etc., forming a self-excited oscillating push-pull circuit. It basically operates as follows: turned-on Vin is applied to the bases of the two NPN triodes through current limiting resistor R1, winding Nb1 and winding Nb2 respectively. Since the parameters of the two triodes are not identical, one of them will conduct first. If triode Q1 conducts first, the magnitude and direction of the transformer flux are determined by the current flowing through collector Q1, and the change in flux will cause an induced electromotive force on the feedback winding that decreases the Vq2 level and increases the Vq1 level. The interaction between the change in flux and the induced electromotive force causes triode Q1 to be subject to saturation conduction and transistor Q2 to be subject to cutoff. At this point, the flux reaches its maximum, and the induced electromotive force, which is proportional to the change rate of the flux, is zero. The disappearance of the induced electromotive force on the feedback winding causes the Vq1 level to drop with the collector current, and the change rate of the current and flux to reverse, leading to the reversal of the induced electromotive force on the feedback winding, the rise of the Vq2 level and the fall of the Vq1 level. The interaction between the change in flux and the induced electromotive force causes triode Q2 to be subject to saturation conduction and transistor Q1 to be subject to cutoff. The above two processes are repeated in cycles, resulting in self-excited oscillations [18].

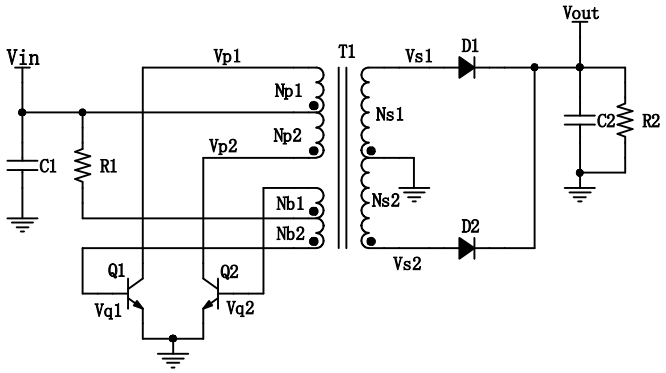

Figure 2. Basic circuit block diagram of Royer converter.

The oscillogram of the basic circuit of a Royer converter is shown in Fig. 3, which shows that the positive feedback oscillation from the collector winding to the base winding forms an Alternating Current (AC) square wave:

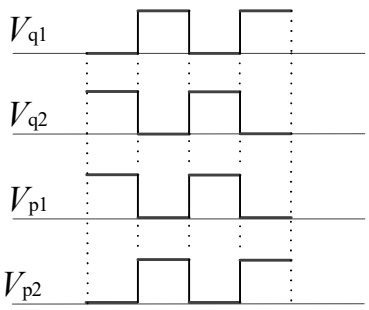

Figure 3. Oscillogram of Royer converter.

Preprints (www.preprints.org) | NOT PEER-REVIEWED | Posted: 29 December 2022 doi:10.20944/preprints202212.0553.v1

The basic circuit of a Royer converter has no feedback control loop. The switch waveform is AC square wave, and there is a large current spike at the moment of transistor cutoff that greatly increases the power consumption of the transistor. The simultaneous existence of high voltage and large current may cause the operating point of the transistor to fail by easily spiking out of the safe operating region. The high-voltage power supply used in air kerma meters should be stable and reliable, so functional circuits can be added to the basic Royer converter circuit and modified to meet the requirements of desired applications. Adding an output feedback loop and oscillation control circuit can stabilize the output voltage; We can reduce the output noise by changing the square wave oscillation to sine wave oscillation ; and decrease the required transformer size by adjusting the output full bridge rectifier circuit to a voltage doubling rectifier circuit.

3. Design of Royer Resonant Circuit

The basic circuit of a Royer converter can be turned into a Royer resonant circuit by adding resonant capacitor C1. In addition, the transformer can be simplified, the center tap of the base control winding can be removed to provide bias voltage at one end of the winding, and the center tap of the high-voltage output winding can also be removed. The presence of the resonant capacitor causes the oscillating circuit to be subject to simple harmonic oscillation at a specific frequency. Frequency f of the oscillation is related to the value of primary inductance L and resonant capacitance C of the transformer coil by the following equation:

$$f = \frac{1}{2\pi}\sqrt{\frac{1}{4LC}} \tag{1}$$

According to the above equation, the Royer resonant circuit generates oscillations at a fixed resonant frequency f. If the oscillation amplitude does not exceed the withstand voltage of the triodes, a standard sine-wave oscillation will be generated, achieving the reduction of output noise [19].

Royer voltage control is designed as auxiliary winding current control, as shown in Fig. 4. It uses a closed-loop negative feedback regulation to control, the emitter or base current of the two push-pull triodes through an error amplifier circuit composed of an operational amplifier, thereby achieving a stable output by controlling the current of the primary or auxiliary winding.

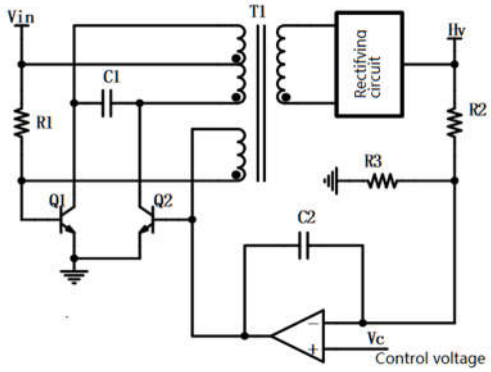

Figure 4. Current control circuit of auxiliary winding.

The secondary winding of transformer T1 outputs Direct Current (DC) high voltage through the rectifier circuit, then divides the voltage through resistors R2 and R3 to obtain sampling voltage and control voltage Vc. The triode base stage current is regulated through the error amplifier circuit. After stabilization by closed-loop negative feedback regulation, output high voltage Hv and control voltage Vc should be subject to the following equations:

$$V_C = H_V \cdot \frac{R_3}{R_2 + R_3} \tag{2}$$

Preprints (www.preprints.org) | NOT PEER-REVIEWED | Posted: 29 December 2022 doi:10.20944/preprints202212.0553.v1

$$H_V = V_C\left(1+\frac{R_2}{R_3}\right) \tag{3}$$

Equation 3 shows that the output high voltage and control voltage are theoretically proportional, and the specific proportion is determined by sampling resistors R2 and R3, but the actual conditions are affected by transformer core saturation. If the control voltage is too high, the output high voltage of the transformer secondary side will be saturated and the output high voltage will remain the same instead of increasing. Closed-loop negative feedback regulation can only be achieved if the control voltage drops back within the range in which the transformer core is not saturated.

In the actual circuit, since sampling resistors R2 and R3 are subject to high voltage, the withstand voltage of a single resistor usually fails to meet the actual demand. Generally, multiple resistors in a series are used for voltage division to ensure that the voltage of each sampling resistor is within the withstand voltage range. In order to increase the maximum output voltage, the core material and size of the transformer can be changed. However, this will increase the size of the circuit board. A voltage doubling rectifier circuit for a diode can also be used to maintain higher output voltage for a smaller circuit board.

4. Test Results

This section provides a concise and precise description of the experimental results, their interpretation, as well as the experimental conclusions that can be drawn.

4.1. Simulation Test Results

4.1.1. Circuit Simulation Test of Flyback Converter

We built the circuit of a flyback converter using the Simulation Program with Integrated Circuit Emphasis (SPICE). The noise of the output high voltage from the flyback converter and the switching signal of the Metal-Oxide-Semiconductor (MOS) tube are observed through two oscilloscope channels, where the observed noise is turned to the AC gear of the oscilloscope. The pulse duty cycle of Pulse Width Modulation (PWM) and the turn ratio of the transformer are adjusted to maintain the output voltage at 300 V. The waveform obtained when the output value is stabilized after 1 ms is shown in shown in Fig. 5.

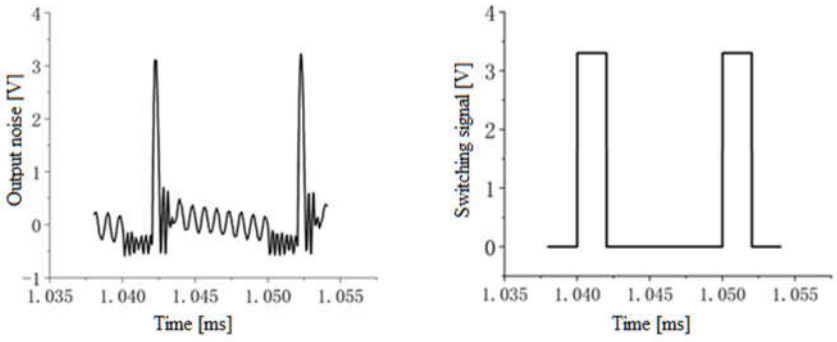

Figure 5. Simulation waveform of flyback converter.

The simulated waveform shows that the output of the flyback converter is severely disturbed at the instant of the MOS tube opening and closing. A pulse with an amplitude of 3.102 V is measured by the oscilloscope of the simulation program to follow the cycle of the switching signal, and the peak-to-peak value of noise at 300 V output is 3.526 V. This indicates that although the structure of the flyback converter is simple, the output noise is very high and will cause a great interference to the measurement results of air kerma meters. As such, is not used as the high-voltage power supply in this study.

Preprints (www.preprints.org) | NOT PEER-REVIEWED | Posted: 29 December 2022 doi:10.20944/preprints202212.0553.v1

4.1.2. Simulation Test of Royer Resonant Circuit

The SPICE simulation program is also used to build a Royer concircuit as shown in Figure 4, in which the rectifier circuit is subject to a voltage doubling rectifier which transforms the sinusoidal AC from the transformer into DC through voltage doubling and rectification. The closed-loop control of the output high voltage can be achieved by varying the control voltage of the error amplifier, wherein sampling resistors R2 and R3 are taken to be 32 MΩ and 100 kΩ, respectively, and the control voltage is 0.3125 V. According to Equation 3, the theoretical value of the output high voltage is 100.3125 V.

Oscilloscope channels A and B in the simulation program are connected to the output high voltage and base voltage of the triodes, respectively, and the waveform obtained by shifting the Y-axis data of the output high voltage by -300 V for easy observation is shown in Fig. 6. In the simulation, the triodes oscillate rapidly and then stop oscillating when the baseline drops to 0. The output high voltage correspondingly rises to its highest point, then begins to fall after the triodes stop oscillating. When the output high voltage falls to near the set value, the triode base starts to oscillate again and generates stable oscillations 0.5 s after the start of the simulation, and the output high voltage is maintained and enters a stabilized state.

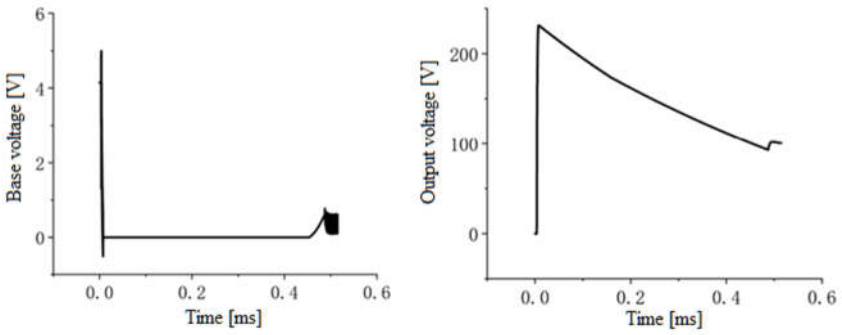

Figure 6. Simulated waveform of Royer resonant circuit.

After the Royer resonant circuit enters the stabilized state, the waveform is selected and amplified to obtain the waveform shown in Fig. 7. It is indicated that the Royer resonant circuit is regulated by closed-loop negative feedback and two triodes can generate stable sinusoidal oscillations after the system is stabilized. The oscillation period measured by the oscilloscope of the simulation program is 10.968 μs, with a frequency of 91.174 kHz. The output high voltage in the stabilized state is 100.282 V which differs very little from the theoretically calculated value. The output high voltage waveform of the simulated Royer resonant circuit is smooth and subject to less noise, making it suitable for the high-voltage power supply of air kerma meters.

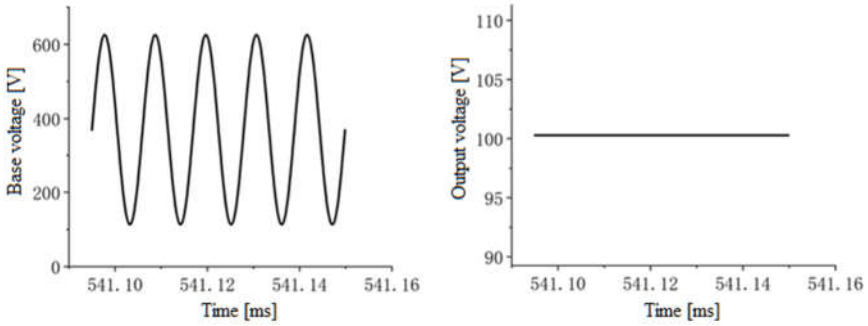

Figure 7. Simulated waveform in stabilized state.

Preprints (www.preprints.org) | NOT PEER-REVIEWED | Posted: 29 December 2022 doi:10.20944/preprints202212.0553.v1

4.2. Performance Test Results

We carry out performance tests in order to evaluate the performance of the developed high-voltage power supply. The tested performance factors include output voltage linearity, linear regulation rate, load regulation rate and output ripple and noise, and the test results and discussions are as follows.

4.2.1. Output Voltage Linearity

The high-voltage power supply is developed and designed to regulate voltage Vadj within the range of 0 to 2.5 V, and the output high voltage is linear and continuously adjustable within the range of 0 to 400 V. The output high voltage is measured by varying the regulating voltage in a step of 0.05 V under the input voltage Vin = 12 V and no-load conditions. The output voltage linearity of the high-voltage power supply is obtained as shown in Fig. 8, and R^2 in the correlation curve is equal to 1. This indicates that the output voltage of the high-voltage power supply shows a good linear relationship with the regulating voltage within the designed operating range.

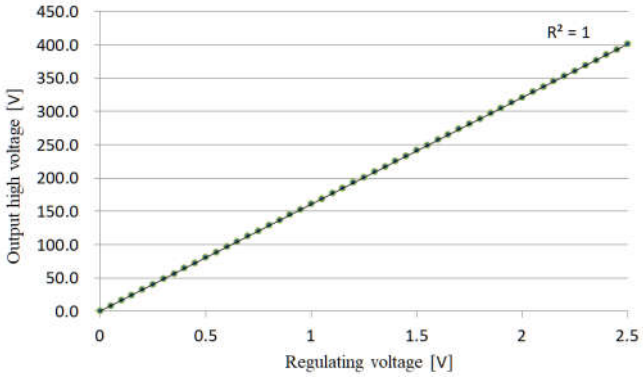

Figure 8. Correlation curve between output high voltage and regulating voltage for high-voltage power supply.

4.2.2. Linear Regulation Rate

Input voltage Vin of the high-voltage power supply proposed herein is designed to operate within the range of 9.6 V-14.4 V. With a regulating voltage of 2.5 V and a load of 400 kΩ, the output high voltage is measured for any large changes by varying the input voltage in a step of 0.2 V. The correlation curve between the output high voltage and input voltage for the high-voltage power supply is shown in Fig. 9. The output high voltage varies by 0.01 V within an input voltage range of 9.6 V -14.4 V with a linear regulation rate of no more than ±0.0025%.

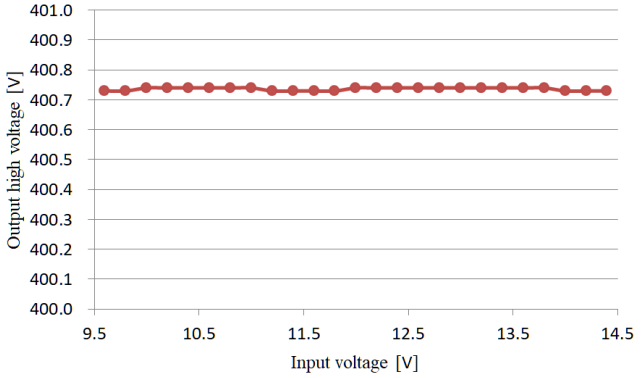

Preprints (www.preprints.org) | NOT PEER-REVIEWED | Posted: 29 December 2022 doi:10.20944/preprints202212.0553.v1

Figure 9. Correlation curve between output high voltage and input voltage for high-voltage power supply.

4.2.3. Load Regulation Rate

The load regulation rate indicates the extent to which the output high voltage of the high-voltage power supply changes as the load changes. The load of the high voltage power supply is designed to be not less than 400 kΩ, and the output high voltage should vary less over the operating range. If the regulating voltage is 2.5 V and the input voltage is 12 V, the output high voltage is measured by varying the load of the high-voltage power supply to generate the correlation curve between the output high voltage and the load for the high-voltage power supply, as shown in Fig. 10, and the load regulation rate is less than ±0.1% within a the load range of 400 kΩ-4,000 kΩ.

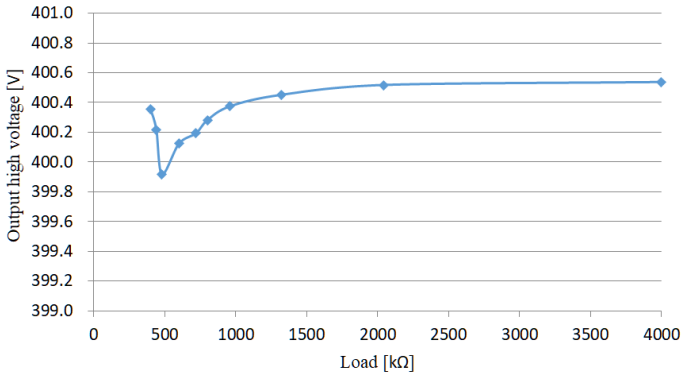

Figure 10. Correlation curve between output high voltage and load for high-voltage power supply .

4.2.4. Output Ripple and Noise

The output ripple and noise of high-voltage power supply restrains the limits of detector measurement, making them particularly important for air kerma meters. With an input voltage of 12 V, regulating voltage of 2.5 V, output high voltage of 400 V and no-load conditions, the output ripple and noise waveform of the high-voltage power supply is measured with the high voltage-resistant oscilloscope probe, as shown in Fig. 11. It can be calculated that the voltage percentage of ripple and noise is less than 0.01%, which meets the design requirements.

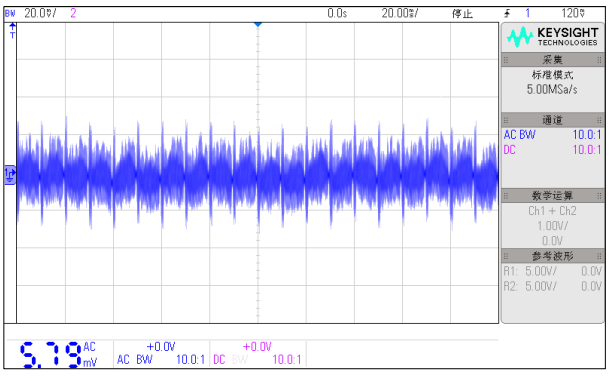

Figure 11. Output ripple and noise waveform of high-voltage power supply.

5. Conclusions

The flyback converter has a simple structure and uncomplicated circuit, and is widely used for switching power supplies, but the results of the SPICE simulation test shows that although the output voltage of the flyback converter enters a stabilized state quickly, the

opening and closing signals of the switch tube disturb the converter and cause it to generate excessive noise. Therefore, the flyback converter is not suitable for use as the high-voltage power supply of air kerma meters. The Royer converter effectively reduces noise by amplifying the stable sinusoidal AC signal from the self-excited push-pull through the transformer, then passing the signal through the rectifier circuit. The closed-loop negative feedback regulation circuit is linearly controlled and, which can achieve the stable control of the output voltage. An adjustable high-voltage power supply is designed according to the principles of the Royer converter, and the Royer resonant circuit is tested by the SPICE simulation program, showing that although its output voltage takes longer to enter the stabilized state, the output high-voltage waveform is smooth and subject to less noise after stabilizing. Actual performance tests indicate that the output voltage linearity, linear regulation rate, load regulation rate, output ripple and noise, and other indexes of the developed adjustable high-voltage power supply meet the requirements and are suitable for air kerma meters.

Author Contributions: Methodology, Jinxing Cheng; software, Qiu Huang; validation, Qingbo Wang, Ai Yu, Weiwei Wen and Youpeng Wu; resources, Jian Yang and Xinyu Li; writing—original draft preparation, Jinxing Cheng ,Fang Liu and Yue Zhang; writing—review and editing, Zeqian Wu； resources,Changwei Zhao. All authors have read and agreed to the published version of the manuscript.

Conflicts of Interest: The authors declare no conflict of interest.

References

1. D.Kwon,M.P.,Little,D.L.,Miller.Reference air kerma and kerma-area product as estimators of peak skin dose for fluoroscopically guided interventions. *Med. Phys.,* 2011, vol.38(7), pp. 4196-4204.
2. N. Ichikawa, A. Fukuda,T Hayash, K. Matsubara. Effect of equalization fifilters on measurements with kerma-area product meter in a cardiovascular angiography system. *J Appl Clin Med Phys*, 2021, vol. 22(12), pp. 177–185.
3. Amendment 2. Medical Electrical Equipment—Part 2–43:" Particular Requirements for the Basic Safety and Essential Performance of X-Ray Equipment for Interventional Procedures,". Geneva, Switzerland: IEC, 2019.
4. A.Malusek, E.Helmrot, M.Sandborg,J.E. Grindborg . Carlsson GA. In-situ calibration of clinical built-in KAP meters with traceability to a primary standard using a reference KAP meter. *Phys Med Biol,* 2014; vol. 59(23), pp. 7195-7210.
5. AQSIQ, "X, γ Radiation Air Kerma (absorbed dose) Rate Meter for Environmental Monitoring," Beijing, 2006.
6. AQSIQ, "(60-250) kV X-ray Air Kerma Meter," Beijing, 2010.
7. M. Imori, T. Taniguchi, H. Matsumoto. Performance of a photomultiplier high voltage power supply incorporating a piezoelectric ceramic transformer. *IEEE Transactions on Nuclear Science*, 2000, vol. 47(12), pp. 2045-2049.
8. G.Q.Zeng , J.Lang , L.Q.Ge , S.L.Wei, J.Yang , K.Q.Zhang. Design of hybrid mode low-noise 3kV high-voltage DC power supply. Atomic Energy Science and Technology, 2016,vol.50 (08), pp. 1510-1516.
9. Q.Guo, Y.Ren, X.R.Guo, G.R.Chang, J.F.Wang. Design of New Programmable High Voltage Power Supply Module. Nuclear Electronics and Detection Technology, 2019, vol.39 (05), pp.545-548.
10. M.J.Qiao , J.Zhang , G.R.Chang , J.Zhang , Y.Liu , X.R.Guo . High voltage circuit design of portable nuclear radiation measurement instrument. *Nuclear Electronics and Detection Technology*, 2016, vol. 36 (08), pp. 781-783.
11. Q.Q.Yu, H.F.Chen, H.Zou, W.H.Shi, J.Q.Zou, W.Y.Zhong. Design of High Voltage Power Supply for New Space Particle Detector. *Nuclear Electronics and Detection Technology,* 2014, vol. 34 (11),pp.1353-1355+1361.
12. S. Feng, L. Shu. Experimental Study of DC High-Voltage Power Supply Ripple. *Nuclear Electronics and Detection Technology,* 2006, vol. 26 , pp. 54-59 .
13. A. Pressman. Switching power supply design. McGraw-Hill Education, 2009.
14. Z.X.Cao, B.H.Lang, Z.R.Yang. Research and design of multi output flyback switching power supply. *Electronic Measurement Technology*, 2020, vol.43 (04),pp. 11-15.
15. H.L.Cheng, Z.C.Zhang, L.F.Jia. Design of a low-power flyback converter. *Power Electronics Technology*, 2018, vol.52 (05),pp.1-4.
16. F.Pan, Q.H.Yang, T.S.Wu. Flyback switching power supply design based on L6562. Power Technology, 2015, vol. 39 (10),pp. 2234-2235+2249.
17. Q.Wang, H.S.Wang, H.W.Tian. Design and simulation of a flyback switching power supply. Computer Simulation, 2021,vol. 38 (04),pp.83-88+138.
18. G.Q. Zeng , L.Q. Ge, W.C. Lai .Design of High-Voltage DC Power Supply for Handheld Radiometer. *Electrical Measurement and Instrumentation.* 2008, vol. 45, pp. 46-49 .
19. X.Y.Liu, G.Q. Zheng. Design of Micro X-ray Tube High Voltage Power Supply Based on Royer Resonance. *NucTe* ,2013, vol. 36, pp. 66-70 .

 doi:10.20944/preprints202212.0553.v1